

PRODUCTION AND ACCELERATION OF IONS

Since the 1950's, growth in our understanding of the interaction of energetic ions with matter has led to some large scale applications of low energy ion beams, for example for materials analysis, semiconductor industry, and materials science. Compact ion accelerators, being the basic technology of the applications, have been developed in a number of embodiments. An accelerator is a device in which charged particles are formed and accelerated to substantial energy. Generally, three primary components are employed: an ion (or electron) source, a beam line, and a target chamber. Ions are produced in an ion source, accelerated to the required energy, transported from the source region to the application region, and finally allowed to bombard the experimental samples in a target chamber. This chapter begins with a description of the basic features of ion implantation into biological samples. Then the working principles of the components of a low-energy accelerator are described as well as the requirements for genetic modification by ion implantation.

2.1. EQUIPMENT REQUIREMENTS FOR ION IMPLANTATION OF BIOLOGICAL SAMPLES

Successful applications of low energy ion beams for genetic modification include ion beam induced mutation for breeding [1,2] and ion beam induced gene transfer [3,4]. In the former case, the ions are required to slow down and finally stop in the genetic substance so that they can cause displacements and recombination of the molecules and atoms of the genetic substance. In the latter case, only ion sputtering and desorption are considered but not the ion penetration range. In other words, ion sputtering or etching thins out the surface of the biological material so that the existing channels can be linked to form the pathways for gene transfer. In fact, ion implantation and etching occur almost simultaneously. An increase in the permeability of the biological material surface enhances deeper penetration of the later coming ions which pass through the channels. Therefore, the ion energy required in ion beam biotechnology is not very high.

For mutation breeding, generally a large number of samples are to be treated. This is not a problem for high-penetration mutation sources such as γ -rays. However, in the case of ion implantation, because of the limited ion range, the ion beam must be caused to

bombard the embryo of each seed. If the beam has a diameter of 30 cm, a maximum of about 3,000 seeds of rice or wheat can be put in this irradiation area even for a very precisely designed sample holder. If the beam size is small, mechanical scanning for large-area homogeneous implantation may cause perturbation of the sample alignment and orientation. Electric or magnetic scanning of the beam is not practical for large implantation areas either. Therefore, the ion beam used for mutation breeding purposes is usually as large and homogeneous as possible.

For studies of ion-beam-induced biological effects, ions are required to be implanted accurately and quantitatively into specific parts of the organisms. Mass spectra of fast ion desorption or photon emission induced by ion impact can be used for measurement of the cell fine structure at the atomic and molecular levels. Particular kinds of ion beams may be used for cell surgery or crafting. All of these applications require the ion beam to have high spatial resolution. Therefore, ion beams applied in the life science should be developed in two extreme directions, namely, high-current broad beams, and micro beams.

In order to avoid loss or scattering of ions due to collisions with gas molecules, the production and acceleration of ions should be carried out in high vacuum. Biological samples, except dry crop seeds, contain a large amount of water. This gives rise to a primary problem. Evaporation of water usually leads to poor vacuum quality, and the biological material can be inactivated by rapid cooling or loss of water. In order to overcome this damage to the bio-samples, careful design of the vacuum system is needed as well as some samples pre-treatment. Additionally, possible contamination from organic materials in the vacuum system from the ion source cathode can occur and should be taken into consideration when designing the ion source.

One possible solution to these dual problems of beam line vacuum and bio-sample survival is to make use of ion beams that are coupled out of the vacuum system. This requires beam energy of at least 2 MeV.

The bio-samples are directly exposed to the ion beam during ion implantation. Thus the design of the sample chamber should guarantee sterile conditions for the plant cells and microbial samples as they are positioned in and removed from the chamber.

2.2. BASIC BEAM LINE STRUCTURE

Although processing of bio-samples calls for some special requirements of the ion beam facility [5,6], the basic structure is not greatly different from that of an industrial ion implanter. Figure 2.1 shows a schematic diagram of a typical accelerator beam line. It consists of the following basic subsystems: (1) ion source; (2) beam focusing system; (3) mass analyzer; (4) accelerating system; (5) measurement system; and (6) target chamber and vacuum system. The components and their arrangement may vary somewhat depending on the specific setup. For example some configurations use pre-acceleration and post-analysis, and the focusing system may be installed at different positions along the beam line according to the ion optics requirements to reduce beam loss.

The working principle is as follows. In the ion source, an electrical discharge in gas or vapor produces plasma. Macroscopically, the plasma is electrically neutral, containing approximately the same amount of positive ion charge as negative electron charge. Ions are extracted from the plasma by an extraction electrode and allowed to drift to a mass

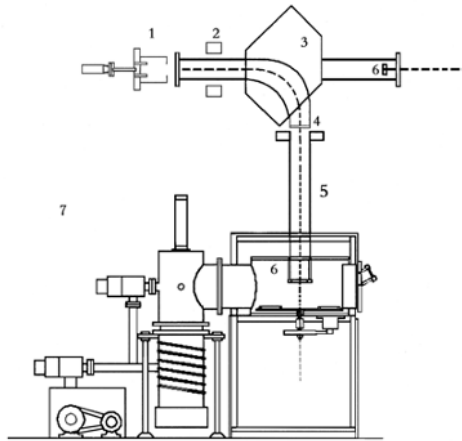


Figure 2.1. Schematic diagram of an ion beam line. (1) Ion source, (2) focusing lens, (3) mass analyzer, (4) diaphragm, (5) accelerating tube, (6) measurement devices, and (7) target chamber and vacuum system.

analyzer. Ions of the same species and with the same charge, selected by the mass analyzer from ions of different masses or charges, go to the acceleration section.

The extraction system accelerates the ions to the selected energy and implants them into the bio-sample inside the target chamber. For monitoring the ion beam parameters, various measurement systems are installed, such as a beam profile monitor and an implantation dose measurement device.

2.2.1. Ion Source

An ion source is a device that produces a beam of ions. It consists of two basic parts – the plasma generator and the ion extraction system. The extraction system is usually composed of two, three or four electrodes. Each electrode has one or several or even several hundred small holes or slits, which are well aligned. The first electrode is at the same potential as the plasma in the discharge chamber, and the last electrode is at ground potential. Figure 2.2 shows a schematic of a two-electrode extraction system. Between the two electrodes a second or third electrode might possibly be added, to form a three- or four- electrode extraction system. Each electrode is biased to the appropriate potential, and ions in the plasma at the boundary of the discharge chamber are accelerated and formed into an ion beam. It is possible for three- or four-electrode extraction systems to form beams of ions with energy up to several hundred keV.

The extraction system forms an ion beam with more-or-less small divergence. A good extractor design can generate an ion beam with divergence less than 0.5° , under optimal conditions. The beam divergence is dependent not only on the arrangement of the extractor optical elements, but also, and usually more importantly, on the density and noise of the plasma near the extraction region. Thus an important factor in reducing the beam divergence is that the plasma density in the discharge chamber is adjusted to match

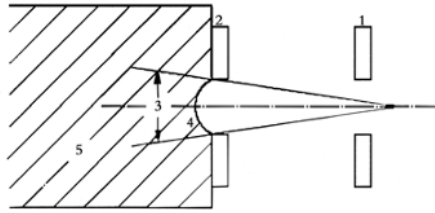


Figure 2.2. Schematic diagram of a dipole extraction system (the shaded part is the plasma). (1) Ground electrode, (2) extraction electrode, (3) effective angle, (4) plasma boundary, and (5) discharge chamber.

that required for the particular the extraction voltage. In first order approximation, the ion beam current density J and the extraction voltage V are related by a 3/2-power-law relationship:

$$J = kV^{3/2}, \quad (2.2.1)$$

where k is a constant dependent on the geometrical parameters of the electrodes and the extracted ion species. Although the value of k can be calculated, it is better determined by experiment. In such an experiment, fixing the extraction voltage V and adjusting the plasma density in the discharge chamber, or fixing the discharge parameters and measuring of the value of J when the beam divergence is the minimum, allows k to be determined from the above equation. In normal operation of an ion source, if the 3/2-power law is satisfied, the divergence of the extracted beam is usually small. In this case the ion beam suffers no significant loss when transported through the beam line.

Ion sources can be classified into two kinds: solid surface ion sources and gas/vapor sources. No matter which type of ion sources is used, formation of a stable discharge is pivotal for good source operation. Many different kinds of ion sources have been developed, such as for example, high-frequency sources, electron cyclotron resonance sources, arc discharge sources, and many more.

2.2.1.1. RF Ion Sources

In an RF (radio frequency) discharge ion source, a high frequency electric field is used to accelerate free electrons to energies that are high enough to lead to ionization of atoms or molecules with which they collide. The plasma chamber may be glass or ceramic, and is surrounded by an RF induction coil fed by high frequency RF power. The RF frequency might be a few MHz up to a few tens of MHz. Gas pressure is typically in the range 0.13 – 1.33 Pa, and a stable plasma can be formed in the discharge chamber. The extraction system forms a more-or-less energetic ion beam from the plasma. The RF ion source has a simple structure and long life. Ions in the beam are mostly (say, ~80%) "atomic ions", meaning that they are ionized atoms as opposed to ionized molecules ("molecular ions"). The basic feed material can be a gas or liquid or solid; liquid or solid feed materials are evaporated in an oven and then enter the discharge chamber as a gas.

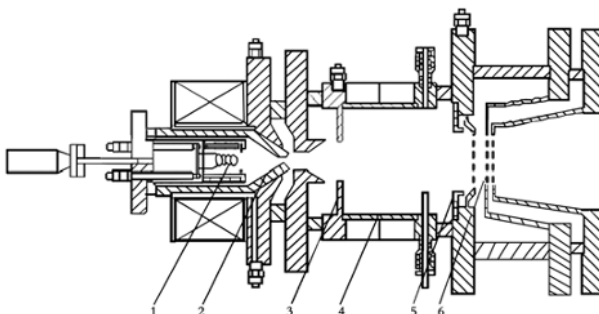


Figure 2.3. Schematic of a duo-Penning ion source. (1) Cathode, (2) intermediate electrode, (3) the first anode, (4) the second anode, (5) target cathode, and (6) extraction system.

2.2.1.2. Duo-Penning Ion Sources

The combination of a duoplasmatron ion source with a Penning discharge is called a duo-Penning ion source (Figure 2.3) [7,8]. The cathode (1) emits electrons which ionize gas in the mid-electrode area (2) to form a plasma. In the mid-electrode area, compression of the plasma by both geometric effects and by a magnetic field causes the plasma to form a double sheath in the throat region. The sheath accelerates the electrons, some of which then have enough energy to pass through the expander of the first anode (3) to enter the anodic discharge chamber (4) in a helical motion along the magnetic field lines. In this way the electron trajectory is lengthened and the collision probability between the electrons and the gas molecules is increased. Since the potential of the target-cathode (5) is lower than that of the anode, the primary electrons are reflected before reaching the cathode and oscillate in the anodic chamber so that the collision probability between the electrons and the gas molecules is yet further increased. The higher ionization efficiency of the anodic chamber gas leads to higher density of the anodic plasma. Ions in the uniform and stable anodic plasma are extracted through the extraction system (6).

The duo-Penning ion source can produce multiply-charged ions. Characteristic features of this type of ion source are high plasma density, stability, and homogeneity. When a multi-aperture extraction system is used, high current and large area ion beams can be formed.

2.2.1.3. ECR Ion Sources

The ECR ion source employs microwave power to supply energy to the electrons in the discharge chamber. When the magnetic field strength is adjusted appropriately, a resonance between the microwave frequency and the electron cyclotron frequency occurs; this is the electron cyclotron resonance, or ECR, condition. Electrons are heated resonantly to high energy, allowing ionization of the background gas by electron collisions. Basic components of the ECR ion source are (1) microwave source (for

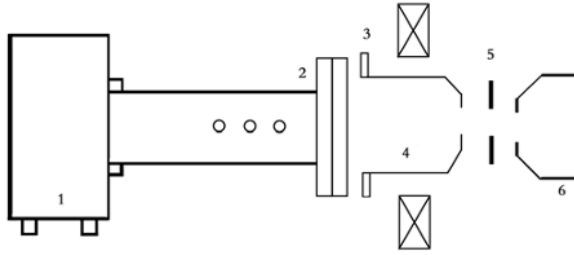


Figure 2.4. Schematic of an ECR ion source. (1) Microwave power supply, (2) microwave input window, (3) magnet, (4) discharge chamber, (5) anode, and (6) extraction electrode.

example, 2.45 GHz), (2) input window, (3) magnetic field, (4) discharge chamber, (5) anode, and (6) extraction electrode (Figure 2.4). This kind of ion source usually operates at low pressures (< 1 Pa) with high ionization efficiency. Because there is no cathode, cathodic sputtering and contamination are avoided and long source lifetime is achieved. Because of the absence of a hot cathode, strongly oxidizing ions can be formed, making this kind of ion source particularly attractive for ion beam bioengineering.

2.2.2. Analysis System

Investigations of biological effects due to different ion species require high purity ion beams [9]. Ions extracted from an ion source are usually a mixture of various components including impurity ions and multiply-charged ions. To purify the beam, mass analysis is employed. The most common kind of mass analysis system employs a magnetic field, which we describe here.

The magnetic analyzer consists of a sector electromagnet and a flat vacuum chamber (Figure 2.5). Ions with mass m , charge q and a velocity v moving in a uniform magnetic field B in a direction perpendicular to the field experience a force, called the Lorentz force, given by

$$\mathbf{F} = q\mathbf{v} \times \mathbf{B}. \quad (2.2.2)$$

The magnitude of the Lorentz force is $F = qvB$, and its direction is perpendicular to both the direction of motion and the magnetic field – hence the ion trajectory is the arc of a circle. The radius of the circle can be obtained from the force balance, $qvB = mv^2/R$, whence

$$R = mv/qB. \quad (2.2.3)$$

If the energy of the ion is W , then $v = (2W)^{1/2}/m$ and the radius of the circular arc can be expressed as

$$R = (2W)^{1/2}/qB. \quad (2.2.4)$$

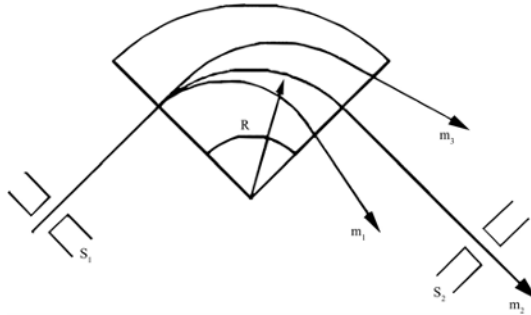


Figure 2.5. Conceptual diagram of a magnetic analyzer.

Since the incident ion energy is $W = qV$, where V is the extraction voltage of the ion source, the beam bending radius can also be expressed as

$$R^2 = 2mV/qB^2. \quad (2.2.5)$$

We see that if the ion charge q , the magnetic field B , and ion energy W are fixed, the ion bending radius depends on its mass m ; and when W , B and m are fixed, the radius depends on the charge number q . Therefore, for a given location of the magnetic analyzer exit (such as the slit S_2 in Figure 2.5), ions of selected mass number or charge number can be extracted. It is usual that magnetic analyzers have a fixed bending radius, thus allowing selection of chosen ion species by adjusting the magnetic field strength B .

2.2.3. Accelerating and Focusing System

The energy at which ions can be extracted from an ion source is limited by high voltage breakdown considerations. For example, for a three-electrode extraction system the upper limit to extraction voltage is about 100 kV. In order to achieve higher ion energies, the ions must be accelerated by an ion accelerating system. For ion bioengineering applications the ion energy typically required is below a few hundred keV, and for this energy range it is convenient to employ an electrostatic accelerating method. The 250 keV (singly charged) ion beam facility designed by the Institute of Plasma Physics, Chinese Academy of Sciences, for ion beam biotechnology uses a double-cylinder accelerating technique, as shown in Figure 2.6. The curves in the figure represent equi-potentials. The electric field E at point A on the left side of the figure, which is perpendicular to the equal-potentials, can be split into a component E_z parallel to the z -axis and a radial component E_r perpendicular to z . When an ion enters this field, it is acted upon by both field components. The field E_z accelerates the ion in the axial direction, while E_r focuses the ion along the axis z . On the right hand side of the central plane M-N, a positive ion diverged from the z -axis due to the E_r component. The ion is accelerated over the entire region. In the field region on the right hand side, the ion speed is higher and the time for which the force acts is shorter. The divergence is small, and hence the overall effect of the field is to form a convergent beam. It should be noted that the second slit is held at negative potential mainly to impede the backflow of electrons.

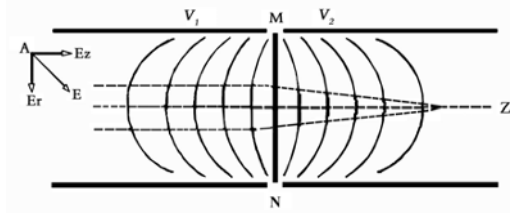


Figure 2.6. Conceptual diagram of a double-cylinder accelerating tube with electrostatic focusing.

This slit plays a divergent role to the positive ions. But, since the potential of this slit is much lower than that of the first slit, the entire system still focuses the ion beam.

If the charge carried by an ion is $q = Ze$, the ion acceleration energy is given by

$$W = q[(V_+ - V_-) + (V_- - V_0)] = q(V_+ - V_0), \quad (2.2.6)$$

where V_+ is the plasma electrode potential, V_- is the accelerating electrode potential and V_0 is the ground potential, or zero,. Thus the ion acceleration energy is given simply by $W = qV_+$.

If a higher ion energy is required, say, greater than several hundred keV, a double-cylinder, single-gap acceleration system is not suitable. Generally, MeV ion energy is produced by a tandem accelerator. The tandem accelerator is one kind of DC high voltage accelerator. The high voltage is applied between two accelerating tubes and both extreme ends of the tubes are grounded. Positive ions are produced in an ion source and converted into negative ions in a charge exchange chamber. The negative ions are accelerated through the first accelerating tube and then stripped of electrons to become positive ions, at the midplane. The positive ions are accelerated again through the second accelerating tube. Thus the ion energy is doubled. A Van der Graaff accelerator (such as that installed at the Institute of Plasma Physics, Chinese Academy of Sciences, and originally from the University of Texas), is an electrostatic accelerator capable of achieving an acceleration energy of 5.5 MeV.

An isolated metal sphere with charge Q and capacitance C will reach a potential given by $U = Q/C$. Addition of charge to the sphere increases the potential U . When the limiting charge is exceeded, a high voltage discharge to the surrounding air will occur. Thus the maximum electric field E_{\max} at the sphere surface should be lower than the discharge voltage E_{disch} , namely $E_{\max} \leq V/r = E_{\text{disch}}$, where r is the sphere radius and V is its voltage relative to ground. The maximum electric field strength that can be supported without breakdown in dry atmospheric air is about 3×10^6 V/m. Thus an acceleration voltage of 3 MV requires a sphere radius of at least 1.0 m. It can be seen that increasing the radius of the metal sphere to increase the acceleration voltage has its limitations. In order to improve the high voltage performance of the accelerator, normally the accelerator is installed inside a steel tank that is filled with a good quality insulating gas. The 5.5 MeV accelerator tank is filled with a mixed gas of 70% N_2 and 30% CO_2 at a pressure of 10–20 atm. The high pressure increases the maximum voltage holdoff, and thus the working voltage of the accelerator. To prevent breakdown, electrostatic accelerators commonly use multiple-stage tubes to distribute the high voltage uniformly

along each stage (Figure 2.7). In this way, although the total voltage of the accelerator is very high the voltage safety coefficient at each stage is sufficient to ensure that breakdown through the air does not occur.

Ions travel a fairly long distance from the ion source to the target chamber. Because of space-charge repulsive forces (Chapter 1), the size of the ion beam increases during beam transport, and there may be a loss of particles from the beam. Scattering due to collisions between ions and residual gas molecules in the beam line can also lead to increased beam size. In order to reduce beam loss as well as to have an appropriately small beam size at the target, the ion beam must be focused. An ion beam can be focused by electric and magnetic fields. The double-tube single-gap accelerator shown in Figure 2.5 is actually a typical electrostatic lens. Ion beam focusing systems that use electrostatic forces are called electrostatic lenses, whereas systems that use magnetic fields are called magnetic lenses. The electro-quadrupole lens and the magnetic quadrupole lens, both of which are strongly focusing lenses, are often used. Lens systems are frequently installed at locations along the beam line for optimal beam focusing according to the ion optics requirements.

2.2.4. Target Chamber and Vacuum System

The target chamber is where the bio-sample is ion-implanted. As opposed to nonliving materials, biological samples are viable and in various shapes, and this can result spatially inhomogeneous ion implantation. In some experiments delivery of the sample into and out of the chamber requires sterile conditions. Thus the design of the chamber and its associated vacuum system must take into account these constraints.

At the present time, ion implantation for mutation breeding requires a large number of samples to be treated. Each individual sample to be implanted should be exposed directly to the ion beam. A vertical ion beam may be preferred for implantation with a beam spot as large and homogeneous as possible. In this way the bio-samples can be ion bombarded with the samples completely motionless. So long as every individual sample is installed in the sample holder in the same orientation, it is guaranteed that the sensitive location of each individual sample is exposed to the ion beam and receives a similar implantation dose.

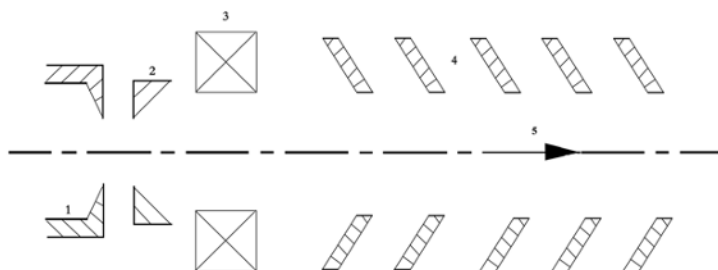


Figure 2.7. Schematic of a multiple-stage accelerating tube. (1) Ion source, (2) extraction electrode, (3) lens, (4) accelerating section, and (5) ion beam.

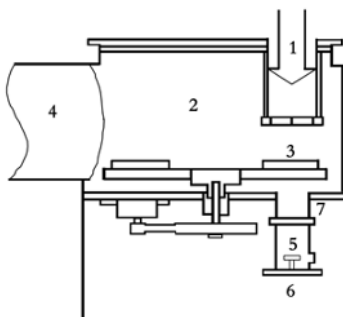


Figure 2.8. Schematic diagram of a target chamber. (1) Ion beam, (2) big target chamber, (3) rotating plate, (4) vacuum pump, (5) small target chamber, (6) sterile chamber, and (7) valve.

Figure 2.8 shows a schematic diagram of a typical target chamber for ion implantation of bio-samples. The ion beam extracted from the ion source and accelerated is incident vertically onto the chamber. The chamber is 90 cm in diameter and 1.0 m in height. A rotating plate 80 cm in diameter is located on the bottom of the chamber. On the plate there are six 20-cm-diameter concave holes, only one of which is completely through. Six 20-cm-diameter sample dishes can be fixed in the concave holes. On the sample dishes there are holes with different diameters for holding various bio-samples. Samples of the same variety, such as rice seeds, are placed in the sample dishes, which are then fixed onto the large rotating plate. The angular position of the plate is adjusted to align one of the dishes with the incident ion beam. After implantation of the first dish, another five sample dishes can automatically be aligned in sequence to the ion beam by computer control, which can also set different implantation parameters. Thus six different sample groups with different implantation parameters can be obtained in a single equipment operation cycle.

Ion implantation of microbes or plant cells is normally carried out in a small target chamber under the main chamber connected by a gate valve. The samples are installed under sterile conditions. The hole on the rotating plate is aligned to the entrance of the small chamber and the valve is then opened to allow ion implantation.

Ion implantation of bio-samples does not require a maximally clean vacuum, and the vacuum produced by a normal oil diffusion pump is adequate. Calculation of the vacuum system should take into account the volume ratio of the large and small chambers so that the small chamber can be pumped down to the desired pressure in a short time. Note that the living bio-samples in the small chamber, that contain a great deal of water, will be rapidly frozen due to pumping of water from the bio-surface, subsequently leading to less water evaporation (see Chapter 4).

2.3. MEASUREMENT OF BEAM CURRENT

Measurement of the ion beam current can be done both electrically and by heat measurements [10]. The electrical method measures total ion charge delivered and then

converts this to a beam current; the heat method measures the heating due to the ion beam and then converts this to a beam current. Often the electrical method is used as a relative measurement, for example to measure the beam current density distribution in the radial direction. If a part of the ion beam is neutralized by background gas collisions during beam transport, the heat measurement may be preferable. The heat power method provides an absolute measurement, and can measure both ions and neutral particles by their energies.

Figure 2.9 shows the principle of the electrical measurement method. Ions pass through a suppression slit and enter a Faraday cup. The ion charge delivered to the cup is measured by the current flow through resistor R , producing a voltage drop V . Thus the ion current can be calculated by

$$I^+ = V/R. \quad (2.3.1)$$

Bombardment of ions on the Faraday cup surface can cause secondary electron emission. This secondary electron current is suppressed by application of a negative voltage.

The thermal measurement method, also called calorimetry, includes adiabatic and non-adiabatic types. Figure 2.10 shows a schematic diagram of an adiabatic calorimeter. When the ion beam bombards the target surface, the kinetic ion energy is transferred to the target internal energy which increases the target temperature. If the metal target has a specific heat C , mass m , initial temperature T_1 , and temperature after one beam pulse T , the energy that the target gains from the ion beam is given by

$$Q = Cm(T - T_1), \quad (2.3.2)$$

and the beam current is

$$I^+ = Q/Vt, \quad (2.3.3)$$

where V is a sum of the extraction voltage and the acceleration voltage (i.e., total applied voltage), and t is the beam pulse length. Thus the target initial temperature T_1 and the temperature after one pulse T are measured, and the beam current can be calculated from (2.3.2) and (2.3.3).

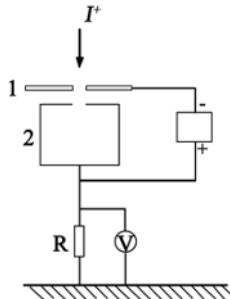


Figure 2.9. Conceptual diagram of electrical measurement. (1) Secondary electron suppression electrode, and (2) Faraday cup.

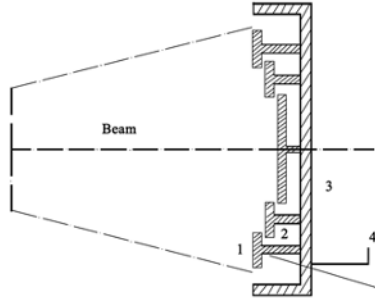


Figure 2.10. Schematic of an adiabatic calorimeter. (1) Partial target, (2) ceramic insulator, (3) screen, and (4) thermocouple.

A metal target has good thermal conductivity. In a long pulse interval, the temperature everywhere on the target surface may be taken to be uniform. Thus the position of the thermocouple that measures the initial target temperature T_1 is not important. Shortly after the target is irradiated with one ion beam pulse, the temperatures at various locations of the target surface will vary. Using of the temperature at one location on the target surface to represent the mean temperature is obviously not reasonable. However, no matter how different the temperatures at different locations of the target surface are, after a relatively long time they will eventually be the same.

If only radiation loss is considered, the temperature change as a function of time after the target reaches an equilibrium temperature is given by

$$\ln[(T - T_0)/(T + T_0)] - 2 \tan^{-1}(T/T_0) = A_1 t + A_0, \quad (2.3.4)$$

where T_0 is the ambient temperature, and A_1 and A_0 are constants to be determined. In the experiment, firstly a number of the pairs (T_i, t_i) are measured based on a certain time interval length, and then the constants A_1 and A_0 are determined using the least-squares method. Eq. (2.3.4) expresses the temperature change after the target reaches an equilibrium temperature. The equivalent mean temperature T instantly after the pulse ends can be obtained from Eq. (2.3.4) with $t = 0$:

$$\ln[(T - T_0)/(T + T_0)] - 2 \tan^{-1}(T/T_0) = A_0. \quad (2.3.5)$$

Substitution the solution for T from Eq. (2.3.5) into Eq. (2.3.2) then provides the beam energy due to one pulse received by the calorimeter.

In ion beam biotechnology experiments, periodic measurement of the ion beam current is necessary. If the ion beam bombardment area is A , the measured beam current I^+ , the implantation time t , and the ions are singly charged, then the implantation dose can be calculated from

$$D = 6.25 \times 10^{18} (I^+/A) t, \quad (2.3.6)$$

where I^+ is in Amperes, A is in cm^2 , and D is in number of ions implanted per cm^2 .

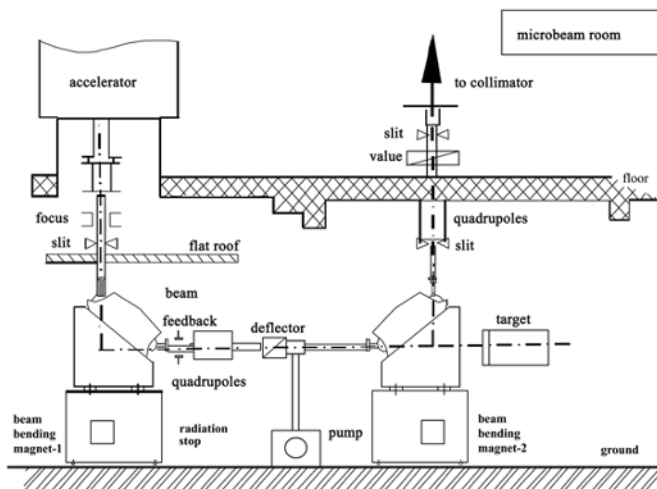


Figure 2.11. Schematic diagram of the ASIPP microbeam line.

2.4 SINGLE-ION MICROBEAM FACILITY

Since the late 1980's, there has been a resurgence of interest in developing and applying single-ion microbeam (SIM) technique [11] to problems in radiation biology [12-17]. One of the studies is on cell and tissue damage caused by ionizing radiations. In this section, SIM facilities will be generally introduced.

A SIM facility mainly consists of an electrostatic accelerator, deflection magnets, beam regulators, quadrupoles, electrostatic deflectors, diaphragms, collimators and so on. A general view of the installation of the ASIPP SIM at the Key Laboratory of Ion Beam Bioengineering, Chinese Academy of Sciences is depicted in Figure 2.11. The microbeam utilizes a CN-5.5 Van de Graaff accelerator, which is able to accelerate singly- or doubly-charged particles, generally produced from a radio-frequency ion source, with the maximum high voltage of 5.5 MV. Accelerated particles of the desired mass and energy are selected using an analyzing magnet which bends the vertical particle beam into a horizontal section of the beam line. Along the beam line is an arrangement of slits, beam feedback, quadrupole magnets and electrostatic steerers, used to define the beam profile and trajectory. The horizontal beam line transports the particles into the second analyzing magnet which bends the beam vertically up to the microbeam experimental room through slits.

SIM, as a new mutation source, is uniquely capable of delivering precisely a predefined number of charged particles (precise doses of radiation) to individual cells or subcellular targets *in situ* normally at an area with a diameter of a few micrometers or smaller. However, even if the beam profile has already been optimized, it is still difficult to confine the beam profile within a desired range such as a diameter of smaller than 1 mm. In order to further reduce the beam size down to an order of micrometer, two methods can be adopted, namely, magnetic focusing and collimation. These two types of

arrangement have some specific technological advantages and some disadvantages respectively. It is clear that a focused arrangement can offer the finest beam and a better defined linear energy transfer (LET) because no particles are scattered inside a collimator [11,18,19]. As an additional bonus, there is more space to install a detector before the target and a higher potential throughput can be gained as the beam line can be deflected to the position of the cells instead of positioning the cells into the beam exit. But a focused arrangement faces more challenges because the focused beam will have to pass through a vacuum window and the cost of installation is considerably greater than a collimated counterpart. On the other hand, there are several advantages by a collimated arrangement. Firstly, there is greater flexibility with regard to the overall configuration of the beam line. This is important, bearing in mind that it is desirable to operate a wet-cell irradiation system vertically. Secondly, collimation offers a straightforward method of reducing the dose-rate to radiobiological levels. Regardless of which method adopted, three crucial factors in general are the high accuracy of targeting, the control of a precise number of charged particles delivered, and high throughput of cells.

A glass capillary collimator is adopted by the ASIPP microbeam to gain a fine beam. A 1 mm long fine bore capillaries with internal diameters as small as $1\text{ }\mu\text{m}$ fits into a stepped hole machined by spark erosion in a 2.1 mm thick stainless steel disk. A $3\text{ }\mu\text{m}$ thick Mylar film is used as a vacuum window. A $7\text{ }\mu\text{m}$ thick aluminum foil and an $18\text{ }\mu\text{m}$ thick scintillator are sandwiched by another $3\text{ }\mu\text{m}$ thick mounting Mylar film. The arrangement of the collimator is illustrated in Figure 2.12. The number of photons emitted and energy consumption will depend on the type and energy of the traversing particle and the total thickness of the thin films used. The number of near-monoenergetic photons emitted is $10^4/\text{s}$ when a $2\sim 3\text{ MeV}$ proton pass through the collimator with the above-described arrangement. A typical energy spectrum from the aligned SIM is shown in Figure 2.13. In practice, the particle number detected will depend on geometry and coupling arrangement of the detector, the quantum efficiency of the detector and other factors, such as losses due to scattering.

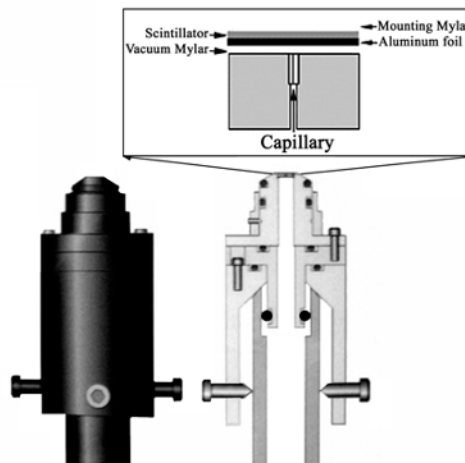


Figure 2.12. The arrangement of the collimator at the ASIPP SIM.

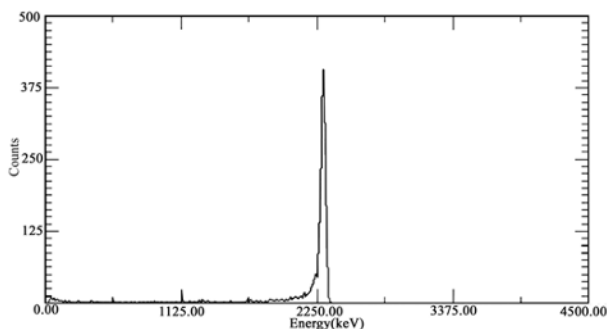


Figure 2.13. The spectrum of 2.2 MeV monoenergetic protons (after passage through the vacuum window and scintillator), collimated by a glass capillary collimator with a 1.0- μm diameter and a 0.98-mm length.

The precision of quantitative radiation and the veracity of localization radiation are the most important technical specifications. To achieve high precision and high veracity of delivery the predefined number of particles to the desired targets, the preconditions that control the key components of the system should be set up. At the same time, diagnosing the active status of the key instruments and promptly evaluating the feedback are necessary to ensure that the experiment is smoothly carried out.

The integrated control system can be divided into three modules logically: imaging acquisition and processing, microscope stage control, and particle counter and beam shutter, as shown in Figure 2.14. The cells to be irradiated are stained and attached to a specific dish. The light spot, which is produced when emitted particles excite the scintillator, can be used as an optical reference to localize the position of the exit aperture. Firstly, the nucleus of each cell is identified and located by a computer/microscope-based image analysis system, which detects the fluorescent staining pattern of the cells by UV light. Secondly, the dish is moved under computer control to the position where the first cell nucleus is positioned over a highly collimated particle beam. The ability to deliver a single or preset number of particles to each cell depends critically on collaborative work of a detector and a beam shutter. During irradiation, the charged particles are detected after passing through the cell. The beam shutter is a fast electrostatic deflection system allowing each irradiated nucleus to be quickly removed from the beam when enough particles have been detected. The beam shutter is opened until the required number of particles has passed through the nucleus. The shutter is then closed, and the next cell is positioned over the beam.

So far, there has been a rapid growth in the number of institutions which are developing SIMs or planning to do so. There are currently more than 14 SIMs worldwide [18,20-37], several SIMs in routine use for radiobiology, and their current major specifications are shown in Table 2.1, and they have been in a constant state of evolution. Much of the recent research using SIMs has been to study low-dose effects and cell signaling, genomic instability, bystander effects and adaptive responses. And the list of possible applications for SIM in radiobiology continues to grow and diversify day by day. Without doubt, scientists don't settle for only targeting nucleus or cytoplasm, and in so doing, cell organelles and tissue becomes the next targets naturally.

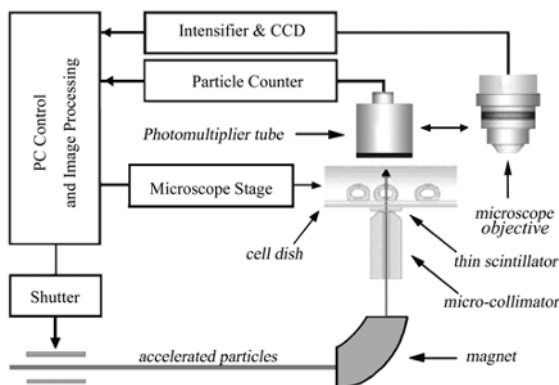


Figure 2.14. Schematic diagram of the overall layout of the ASIPP microbeam facility and the integrated control system.

SIMs have been in constant development and much progress has been made over the past few years. For example, a laser ion source (LIS) enables us to use ions of sufficient range from hydrogen to iron and provide a wider range of LET [38,39]. However, a number of aspects of SIM performance should continue to be scrutinized and if possible, improvements should be implemented, such as increasing the cell throughput, increasing the target accuracy, increasing the penetration of the irradiation and applying non-UV methods for target visualization. The throughput of the SIM needs to further increase because statistical uncertainty and the low incidence of some biological endpoints (e.g. the expression of genes in terms of a cell population in general comes from samples involving millions of cells). And the combination of pre-cell detection and post-cell detection may be the only way to eliminate the possibility of overcount or undercount. Only in this way, SIM could meet the need of mountainously growing applications in biology.

SIM, as a powerful tool, opens up the possibility of probing the answers to many enigmas in radiobiology, but some new technologies should be grafted in or related by marriage. Provided that visual observation of the cells and particle detection occur simultaneously (lucite light guide technique provides an elegant solution for this intent), different technologies could bring out the best in each other. Many optical screening technologies would be expected to be contributors, notwithstanding cell-based applications in high throughput screening (HTS) form a considerable challenge to both instrumental design and fully automated data handling and evaluation, especially the miniaturized HTS and ultra-HTS (uHTS) at ambient temperature. Most importantly, they open up the possibility to online *in situ* physiological monitoring the cells or tissues in a noninvasive way [40]. In doing so, scientists could fix attention on the original process of the interaction between low-energy ions and complicated organisms rather than endpoints, and gain deeper insight into the true nature. Fortunately, biologists and biophysicists are now joining forces to bring major advances in the art of SIM. It is believed that this is not the end of the saga.

Table 2.1. SIMs worldwide in routine use and their current main specifications.

Institution	SIM	Accelerator	Particles	Energy /LET	Mode of detection	Targeting accuracy	Through-put
RARAF, Columbia University, USA	RARAF micro-beam	4.2MeV Van de Graaff accelerator	From hydrogen to iron	10 - 4500 keV/ μm	Gas-filled ionization chamber and a SSD detector	$\sim \pm 2\mu\text{m}$	$\sim 11,000$ cells per hour
CRC Gray Laboratory, Northwood, UK	GCI micro-beam	4MeV Van de Graaff accelerator	Protons, Helium ions	5.7MeV He^3	Scintillator + PMT	$< \pm 2\mu\text{m}$	$\sim 36,000$ cells per hour
JAERI-Takasaki, Japan	TIARA micro-beam	AVF-cyclotron accelerator	From C ions to Fe ions	8-1800 keV/ μm	a CaF_2 (Eu) scintillator + PMT	$\sim \pm 1\mu\text{m}$	$> 60,000$ cells per hour
CENBG, Bordeaux, France	CENBG micro-beam	4MeV Van de Graaff accelerator	Protons, Helium ions	3.5MeV alpha or proton	a thin scintillating foil + Gas transmission detector	$\pm 2\mu\text{m}$	$> 2,000$ cells per hour
PTB, Braunschweig, Germany	PTB micro-beam	3.75 MeV Van de Graaff and 20–35MeV cyclotron accelerators	Protons, Helium ions	3 - 200 keV/ μm	Scintillator + PMT	$\pm 1.5\mu\text{m}$	15,000 cells per day
NIRS, Chiba, Japan	SPICE micro-beam	HVEE Tandem accelerator	Protons, Helium ions	3.4 MeV H^+ , 5.1 MeV He^{2+}	Scintillator + PMT	$< \pm 2\mu\text{m}$	2,000 cells per hour
University of Melbourne, Parkville, Australia	MARC Micro-beam	5U NEC Pelletron accelerator	Protons, Helium ions, C, N, O	4.6~7.7 MeV alpha particles	Boron doped thin diamond film + SSD + CEM detector	$\leq \pm 300\text{nm}$	$> 3,000$ cells per hour
IPP, CAS, Hefei, China	CAS-LIBB micro-beam	5.5 MV Van de Graaff accelerator	$^1\text{H}^+$, $^2\text{H}^+$	3.5 MeV H^+ , 3.5 MeV $^2\text{H}^+$	Scintillator + PMT	$\sim \pm 1\mu\text{m}$	-
MIT LABA, Boston, USA	MIT LABA micro-beam	1.5 MV single stage electrostatic accelerator	He^{2+} , H^+ , He^+	15-30 keV/ μm	Light guide + plastic scintillator + PMTs	$\sim \pm 3\mu\text{m}$	-
GSI, Darmstadt, Germany	SIHF micro-beam	GSI linear accelerator (UNILAC)	From Carbon to Uranium	1.4MeV/ μm – 11.4 MeV/ μm	Si_3N_4 foil + channeltron	$< \pm 1\mu\text{m}$	-
Technische Universität München, Germany	SNAKE micro-beam	14MV Munich Tandem accelerator	From protons to uranium	2 KeV/ μm – several MeV/ μm	Position-sensitive detector (PSD)	$\sim \pm 700\text{nm}$	-
University of Leipzig, Leipzig, Germany	LIPSION micro-beam	3.5 MV Singletron TM accelerator	Protons, Helium ions	10-20 keV/ μm	Multi-detector	$\sim \pm 130\text{nm}$	-
WERC, Japan	W-MAST micro-beam	5 MV tandem accelerator	Protons	10 MeV proton	Si surface-barrier detector (SSD)	$\sim \pm 10\mu\text{m}$	-
INFN-LNL, Padova, Italy	INFN micro-beam	7MeV Van de Graaff CN accelerator	$^1\text{H}^+$, $^2\text{H}^+$, $^3\text{He}^{2+}$, $^4\text{He}^{2+}$	7-150 keV/ μm	Silicon detector	-	-

REFERENCES

- 1 Yu, Z.L., Deng, J.G. and He, J.J., Mutation Breeding by Ion Implantation. *Nucl. Instr. Meth.*, **B59/60** (1991)705-708.
- 2 Wu, L.F. and Yu, Z.L., Radiobiological Effects of a Low-energy Ion Beam on Wheat, *Radiat Environ Biophys*, **40** (2001)53–57.
- 3 Yu, Z.L., Ion Beam Application in Genetic Modification. *IEEE Trans. on Plasma Sci.*, **28** (2000)128-135.
- 4 Yu, Z.L., Yang, J.B., Wu, Y.J., *et al.*, Transferring Gus Gene into Intact Rice Cells by Low Energy Ion Beam, *Nucl. Instr. Meth.*, **B80/81** (1993)1328-1331.
- 5 Yu, Z.L., Ion Beam and Biology Science, *Physics* (Chinese), **26** (1997)333–338.
- 6 Yu, Z.L., Interaction between Low Energy Ions and the Complicated Organism, *Plasma Sci. & Tech.*, **1** (1999) 79-85.
- 7 Yu, Z.L., He, J.J., Zhou, J. and Deng, J.G., High-Current DC Ion Source with Large Radiation Area, *Vacuum Science and Technology*, **9**(6) (1989)379–382.
- 8 Yu, Z.L., Xu, P., He, J.J., Gao, S.Q. and Zhou, J., Studies on IS-A 10cm-Duopigatron Ion Source, *Chinese Journal of Nuclear Science and Engineering*, **7**(3,4) (1987) 318–321.
- 9 Yu, Z.L., Xu, P., He, J.J. and Zhou, J., Experiments and Applications of IS-A Type Duopigatron, *Nuclear Technology*, **12**(10) (1989)614–617.
- 10 Yu, Z.L., Power Measurements of Heavy Current Pulsed Ion Beam, *Nuclear Technology*, **12**(4) (1989)205–208.
- 11 Watt, F. and Grime, G.W., *Principles and Applications of High Energy Ion Microbeams* (Adam Hilger, Brostol., 1987).
- 12 Zirkle, R.E and Bloom, W., Irradiation of Parts of Cells, *Science*, **117**(1953)487–493.
- 13 Bloom, W., Cellular Responses, *Rev. Modern Phys.*, **31**(1959)66–71.
- 14 Legge, G.J.F., A History of Ion Microbeams, *Nucl. Instr. Meth.*, **B130** (1997)9–19.
- 15 Brenner, D.J. and Hall, E.J., Microbeams: A Potent Mix of Physics and Biology, *Radiat. Prot. Dosim*, **99**(2002)283–286.
- 16 Hei, T.K., Wu, L.J., Liu, S.X., *et al.*, Mutagenic Effects of a Single and an Exact Number of α Particles in Mammalian Cells, *Proc. Natl. Acad. Sci. USA*, **94** (1997)3765–3770.
- 17 Wu, L.J., Randers-Pehrson, G., Xu, A., *et al.*, Targeted Cytoplasmic Irradiation with Alpha Particles Induces Mutations in Mammalian Cells, *Proc. Natl. Acad. Sci. USA*, **96**(1999)4959 ~ 4964.
- 18 Cholewa, M., Saint, A., Legge, G.J.F., *et al.*, Design of a Single Ion Hit Facility, *Nucl. Instr. Meth.*, **B130**(1997)275–279.
- 19 Sakai, T., Naitoh, Y., Kamiya, T., *et al.*, Single Ion Hitting to Living Samples. *Nucl. Instr. Meth.*, **B158**(1999)250–254.
- 20 Folkard, M., Vojnovic, B., Prise, K.M., *et al.*, A Charged-Particle Microbeam: I. Development of an Experimental System for Targeting Cells Individually with Counted Particles, *Int. J. Radiat. Biol.*, **72** (1997)375–385.
- 21 Folkard, M., Vojnovic, B., Hollis, K.J., *et al.*, A Charged-Particle Microbeam: II. A Single-Particle Micro-Collimation and Detection System, *Int. J. Radiat. Biol.*, **72** (1997)387–395.
- 22 Dymnikov, A.D., Brenner, D.J., Johnson, G., *et al.*, Theoretical Study of Short Electrostatic Lens for the Columbia Ion Microprobe, *Rev. Sci. Instr.*, **71**

- (2000)1646-1650.
- 23 Butz, T., Flaggmeyer, R-H., Heitmann, J., *et al.*, The Leipzig High-Energy Ion Nanoprobe: A Report on First Results, *Nucl. Instr. Meth.*, **B161-163**(2000)323- 327.
 - 24 Fischer, B.E., Cholewa, M. and Hitoshi, N., Some Experiences on the Way to Biological Single Ion Experiments, *Nucl. Instr. Meth.*, **B181**(2001)60–65.
 - 25 Randers-Pehrson, G., Geard, C.R., Johnson, G., *et al.*, The Columbia University Single-Ion Microbeam, *Radiat. Res.*, **156**(2001)210–214.
 - 26 Michelet, C., Moretto, Ph., Barberet, Ph., *et al.*, A Focused Microbeam for Targeting Cells with Counted Multiple Particles, *Radiat. Res.*, **158**(2002)370–371.
 - 27 Dollinger, G., Datzmann, G., Hauptner, A., *et al.*, The Munich Ion Microprobe: Characteristics and Prospect, *Nucl. Instr. Meth.*, **B210** (2003)6–13.
 - 28 Greif, K. D., Brede, H. J., Giesen, U., *et al.*, The PTB Focused Microbeam for High and Low LET Radiation, *Radiat. Res.*, **161**(2004)89–90.
 - 29 Oikawa, M., Kamiya, T., Fukuda, M., *et al.*, Design of a Focusing High-Energy Heavy Ion Microbeam System at the JAERI AVF Cyclotron, *Nucl. Instr. Meth.*, **B210**(2003)54-58.
 - 30 Cholewa, M., Fischer, B. E. and Heiß, M., Preparatory Experiments for a Single Ion Hit Facility at GSI, *Nucl. Instr. Meth.*, **B210**(2003)296–301.
 - 31 Folkard, M., Vojnovic, B., Gilchrist, S., *et al.*, The Design and Application of Ion Microbeams for Irradiating Living Cells and Tissues, *Nucl. Instr. Meth.*, **B210** (2003)302-307.
 - 32 The Radiological Research Accelerator Facility, *RARAF Annual Report 2002*, Columbia University, USA.
 - 33 Wu, L.J., Hei, T.K., Randers-Pehrson, G., Wang, S.H., and Yu, Z.L., Columbia University Microbeam: Development of an Experimental System for Targeting Cells Individually with Counted Particles, *Nucl. Sci. and Tech.*, **10**(3)(1999).
 - 34 Hu, Z.W., Yu, Z.L. and Wu, L.J., An Optimization Control Program for the ASIPP Microbeam, *Nucl. Instr. Meth.*, **A507**(2003)617–621.
 - 35 Wang, X.F., Chen, L.Y., Hu, Z.W., Wang, X.H., Zhang, J., Li, J., Wu, L.J., Wang, S.H., Yu, Z.L., *et al.*, Quantitative Single-Ion Irradiation by ASIPP Microbeam, *Chin. Phys. Lett.*, **21**(2004)821–824.
 - 36 Moretto, Ph., Michelet, C., Balana, A., *et al.*, Development of a Single Ion Irradiation System at CENBG for Applications in Radiation Biology, *Nucl. Instr. Meth.*, **B181**(2001)104–109.
 - 37 Cherubini, R., Conzato, M., Galeazzi, G., *et al.*, Light-Ion Microcollimated Beam Facility for Single-Ion, Single Mammalian Cell Irradiation Studies at LNL-INFN, *Radiat. Res.*, **158**(2002)371– 372.
 - 38 Bigelow, A.W., Randers-Pehrson, G. and Brenner, D.J., Laser Ion Source Development for the Columbia University Microbeam, *Rev. Sci. Instr.*, **73** (2002)770-772.
 - 39 Bigelow, A.W., Randers-Pehrson, G. and Brenner, D.J., Proposed Laser Ion Source for the Columbia University Microbeam, *Nucl. Instr. Meth.*, **B210**(2003)65-69.
 - 40 Nelms, B.E., Maser, R.S., MacKay, J.F., *et al.*, *In Situ* Visualization of DNA Double-Strand Break Repair in Human Fibroblasts, *Science*, **280**(1998)590-592.

FURTHER READING

1. Brown, I.G., ed. *The Physics and Technology of Ion Sources*, 2nd Edition, (Wiley-VCH, Berlin, 2004).
2. Ivanov, B.H. and Razov, B.H., *Fundamentals of Micro-Dosimetry*, transl.: Hua, M.C. (in Chinese, Atomic Energy Press, Beijing, 1987).
3. Nastasi, M., Mayer, J.W. and Hirvonen, J., *Ion-Solid Interactions: Fundamentals and Applications* (Cambridge University Press, Cambridge, 1996).
4. Wang, Y.H., *et al.*, *Fundamentals of Ion Implantation and Analysis* (in Chinese, Aviation Industry Press, Beijing, 1992).
5. Zhang, G.H. and Zhong, S.L., *Ion Implantation Technology* (in Chinese, Engineering Industry Press, Beijing, 1982).
6. Zhu, R.S., *Principles and Applications of Solid Nuclear Trace Detectors* (in Chinese, Science Press, Beijing, 1987).
7. Ziegler, J.F., ed. *Ion Implantation: Science and Technology* (Academic Press, New York, 1984).



<http://www.springer.com/978-0-387-25531-6>

Introduction to Ion Beam Biotechnology

Yu, Z.

2006, XIX, 287 p., Hardcover

ISBN: 978-0-387-25531-6